

---

# Laser Transponders for High-Accuracy Interplanetary Laser Ranging and Time Transfer

John J. Degnan

Sigma Space Corporation, 4801 Forbes Blvd., Lanham, MD 20706 USA

**Summary.** Satellite laser ranging (SLR) and lunar laser ranging (LLR) to passive reflectors have been carried out successfully since 1964 and 1969, respectively. The single-ended SLR ranging technique, although capable of providing millimeter precision range data to satellites, is not practical over interplanetary ranges. Double-ended laser transponders for decimeter or better accuracy interplanetary ranging and subnanosecond time transfer are well within the state-of-the-art, however, as was recently demonstrated in two successful transponder experiments carried out by the NASA Goddard Space Flight Center to laser altimeters onboard the Messenger spacecraft (currently enroute to Mercury) and the Mars Global Surveyor spacecraft (presently in Mars Orbit). A high-accuracy interplanetary ranging capability would support a number of new scientific investigations (e.g., solar system and planetary physics, general relativity, etc.) and enhance deep-space mission operations and reliability through vastly improved navigation accuracy and time synchronization with Earth mission control centers. The performance of future lunar or interplanetary laser transponder and laser communications instruments can be simulated and tested at distances to Pluto and beyond using existing passive SLR and LLR targets already in space.

## 1 Satellite and Lunar Laser Ranging

Laser ranging to passive retroreflectors on Earth orbiting satellites was first demonstrated at the NASA Goddard Space Flight Center on 31 October 1964 [8]. The basic measurement of this single-ended instrument is both simple and unambiguous. The outgoing laser pulse starts a highly precise timer, is reflected by the satellite, and the return signal stops the timer. One then multiplies the time interval by the speed of light, correcting for satellite signature (impulse response) and atmospheric propagation delay effects, to compute a range to the satellite center of mass. Today, an international network of approximately 40 satellite laser ranging (SLR) stations routinely track two dozen space missions in Earth orbit. Over the past four decades, the ranging precision has improved from a few meters to 1 or 2 mm, and the subcentimeter

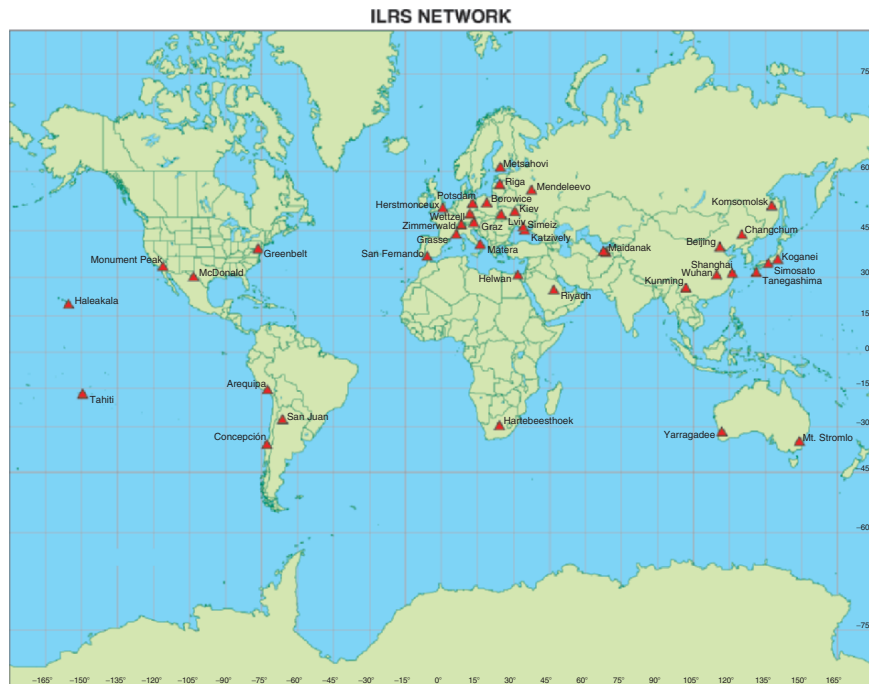


**Fig. 1.** Global distribution of the ILRS satellite laser ranging network.

absolute accuracy is presently limited, not by the instrumentation, but by uncertainties in the atmospheric propagation model and pulse spreading by the satellite target arrays. For more information on SLR, the reader is referred to a series of review articles devoted to SLR history [3], hardware [1], and mathematical models [2].

Since its inception in 1998, the International Laser Ranging Service (ILRS), an Official service of the International Association for Geodesy (IAG), has set mission tracking policy and managed the daily operations of the international SLR network. The global distribution of ILRS stations is shown in Fig. 1, and, as will be demonstrated later, most of these stations are potentially capable of supporting future centimeter ranging and subnanosecond time transfer to the other planets within our solar system.

A select few of the ILRS stations have successfully tracked one or more of the five retroreflectors placed on the Moon by the manned US Apollo 11, 14, and 15 and two unmanned Soviet Lunakhod missions to the Moon. Most of the operational lunar laser ranging (LLR) data over the past 36 years has come from three sites – the NASA/University of Texas station at McDonald Observatory, the French CERGA station in the coastal Mediterranean town of Grasse, and the NASA/University of Hawaii station at the top of Mt. Haleakala in Maui (which was decommissioned in 1992 due to NASA funding

cuts). It is important to note that, even with meter class telescopes located at mountaintop sites with excellent atmospheric “seeing” and with moderately high subnanosecond pulse energies on the order of 100–200 mJ, LLR systems typically detect one single photon return from the lunar arrays out of every 10–20 laser fires, or roughly one photon per second at typical 10–20 Hz fire rates. This low signal photon return rate makes the extraction of the signal from background noise difficult except when the sunlit lunar surface is outside the receiver field of view (FOV). On the other hand, LLR observers have also found it necessary to offset their pointing from prominent lunar features to guide their narrow laser beam successfully to the target. The net consequence of these two constraints is to limit lunar tracking to temporal periods which are far from both “Full Moon” and “New Moon.” In spite of these limitations, LLR has proved invaluable to a number of important scientific endeavors in the fields of lunar physics and general relativity [6]. These include:

*Lunar Physics (LLR)*

- Centimeter accuracy lunar ephemerides
- Lunar librations (variations from uniform rotation)
- Lunar tidal displacements
- Lunar mass distribution
- Secular deceleration due to tidal dissipation in Earth’s oceans
- Measurement of  $G(M_E + M_M)$

*General Relativity*

- Test/evaluation of competing theories
- Support atomic clock experiments in aircraft and spacecraft
- Verify equivalence principle
- Constrain  $\beta$ -parameter in the Robertson–Walker metric
- Constrain time rate of change in  $G$

Under the Apache Point Observatory Lunar Laser-ranging Operation (APOLLO) program in New Mexico, activities have been underway to produce multiphoton lunar ranging returns through the use of larger 3.5 m diameter telescopes and more powerful lasers [7], and the first lunar returns were reported in October 2005.<sup>1</sup> Returns from both the strongest (Apollo 15 with 300 retroreflectors) and weakest (Apollo 11 with 100 retroreflectors) lunar targets were obtained including some successful experimental sessions near Full Moon. During the best run reported to date, 420 returns were detected out of 5,000 attempts for an 8.4% return rate. Nevertheless, the conventional SLR technique of ranging to passive retroreflectors is unlikely to be useful for targets much beyond the Earth–lunar distance (384,000 km or 0.0026 AU). This is due to the  $R^{-4}$  dependence of the received signal strength, where  $R$  is the target range.

<sup>1</sup> [http://physics.ucsd.edu/~tmurphy/apollo/first\\_range.html](http://physics.ucsd.edu/~tmurphy/apollo/first_range.html)

## 2 Science and Mission Benefits of Interplanetary Ranging

Transponders can overcome the distance limitations of conventional SLR and LLR systems. Transponders consist of two terminals – each with its own laser, telescope, and timing receiver [5]. Their principal advantage is that the signal strength falls off only as  $R^{-2}$ , and this greatly extends the range over which they can be used. The possibility of interplanetary ranging at the centimeter level provides new measurement opportunities in the fields of solar system and planetary science and general relativity. It also provides new operational capabilities, which can reduce the risk and cost of navigating and monitoring future spacecraft missions. Some examples follow:

### *Solar System and Planetary Science*

- Solar physics: gravity field, internal mass distribution, and rotation
- Few millimeter accuracy lunar ephemerides and librations
- Improves ranging accuracy and temporal sampling over current LLR operations to Apollo retroreflectors on the Moon with small, low energy, ground stations
- Decimeter or better accuracy planetary ephemerides
- Mass distribution within the asteroid belt

### *General Relativity*

It provides more accurate (2–3 orders of magnitude) tests of relativity and constraints on its metrics than LLR or microwave radar ranging to the planets, e.g.:

- Precession of Mercury’s perihelion
- Constraints on the magnitude of  $\dot{G}$  ( $1 \times 10^{-12}$  from LLR)
- Gravitational and velocity effects on spacecraft clocks
- Shapiro time delay

### *Lunar and Planetary Mission Operations*

- Decimeter or better accuracy spacecraft ranging
- Calibration/validation/backup for Deep Space Network (DSN) microwave tracking
- Subnanosecond transfer of GPS time to interplanetary spacecraft; for improved synchronization of Earth/spacecraft operations
- Transponder can serve as independent self-locking beacon for collocated laser communications systems

### 3 Echo vs. Asynchronous Transponders

There are two types of transponder: *echo* and *asynchronous*. The timing diagrams for echo and asynchronous transponders are shown in Fig. 2a,b, respectively. In an Earth–Moon echo transponder, for example, a pulse emitted from the Earth terminal at time  $t_{E1}$  is detected by the lunar terminal at time  $t_{M1}$  which then generates a response pulse at time  $t_{M2}$  subsequently detected by A at time  $t_{E2}$ . The delay between the received and transmitted pulse at the lunar terminal,  $t_d$ , would be either known a priori through careful calibration or controlled via active electronics and would be subtracted from the observed round-trip time before computing the target range. Alternatively, the delay can be measured locally by a timer at the lunar terminal and transmitted to the Earth terminal via a communications link. The signal return rate at the primary station is then equal to the fire rate of the laser multiplied by the joint probability that pulses are detected at both ends of the link. Thus, the simple echo approach works very well when the round-trip time-of-flight is relatively short and there is a high probability of detection at both ends of the link, i.e., when both the uplink and downlink signal is reasonably strong and pointing uncertainties are small relative to the transmitter divergence. This approach should work very well over Earth–Moon or shorter links. However, in interplanetary links where the light transit time is relatively long (several

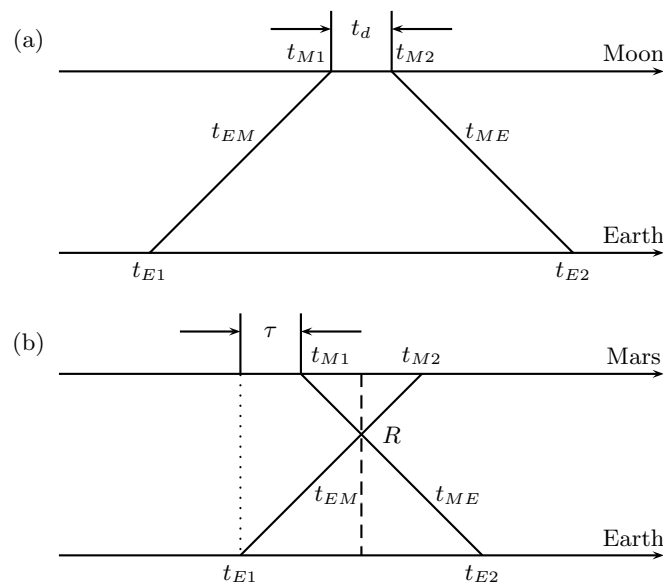


**Fig. 2.** Timing diagrams for (a) echo and (b) asynchronous transponder.

minutes to hours) and the probability of detection is small at one or both ends of the link, it is worthwhile considering the asynchronous laser transponder.

In an asynchronous transponder, the two terminals independently fire pulses at each other at a known laser fire rate, as illustrated by the timing diagram in Fig. 2b. For an Earth–Mars link, for example, the Earth terminal records the times of departure of its own transmitted pulses ( $t_{E1}$ ) as well as the times of arrival of pulses from Mars ( $t_{E2}$ ) and vice versa. In a high SNR system with good pointing, the pulses arrive at roughly the laser fire rate whereas, in low Signal-to-Noise Ratio (SNR) or photon-counting systems [5], the pulses may arrive intermittently. The departure and arrival times measured at each terminal are then communicated to, and properly paired at, an Earth-based processor which then calculates a range and clock offset between the two terminals for each set of two-way measurements occurring within a reasonably short time interval. The relevant equations are

$$R = \frac{c}{2}[t_{ME} + t_{EM}] = \frac{c}{2}[(t_{E2} - t_{E1}) + (t_{M2} - t_{M1})] \quad (1)$$

for the inter-terminal range at the time when the two photon world lines cross in Fig. 2b and

$$\tau = \frac{(t_{E2} - t_{E1}) - (t_{M1} - t_{M2})}{2(1 + \dot{R}/c)} \quad (2)$$

for the corresponding time offset between the pulses departing from each terminal, where  $\dot{R}/c$  is a correction for the range rate between the two terminals.

For a more extensive discussion of the theory of laser transponders, background noise and error sources, proposed methods for terminal and signal acquisition, and detailed analyses of an Earth–Mars link, the reader is referred to a comprehensive article previously published by Degnan [5]. The remainder of the present chapter will concentrate on new insights gained by comparisons with the SLR effort and on recent experiments that clearly demonstrate that interplanetary laser transponders are well within the present state-of-the-art.

## 4 Recent Deep-Space Transponder Experiments

In late May 2005, NASA Goddard Space Flight Center (GSFC) was conducting the first successful two-way transponder experiments at a wavelength of 1,064 nm with a laser altimeter onboard the Messenger spacecraft, which is currently enroute to Mercury. From a distance of about 24 million km (0.17 AU), the Messenger spacecraft performed a raster scan of the Earth while firing its Q-switched Nd:YAG laser at an 8 Hz rate. Simultaneously, a ground based Q-switched Nd:YAG laser at GSFC's 1.2 m telescope was aimed at the Messenger spacecraft. During the few second periods when the Messenger raster scan passed over the Earth station, pulses were successfully exchanged between the two terminals [10]. The pulse time of departure and

**Table 1.** Summary of key instrument parameters for recent deep-space transponder experiments at 1,064 nm.

Experiment	MLA (cruise)		MOLA (Mars)
Range ( $10^6$ km)	24.3		$\sim 80.0$
Wavelength (nm)	1,064		1,064
	Uplink	Downlink	Uplink
Pulse width (ns)	10	6	5
Pulse energy (mJ)	16	20	150
Repetition rate (Hz)	240	8	56
Laser power (W)	3.84	0.16	8.4
Full divergence ( $\mu$ rad)	60	100	50
Receive area ( $m^2$ )	0.042	1.003	0.196
EA-product ( $J m^{-2}$ )	0.00067	0.020	0.0294
PA-product ( $W m^{-2}$ )	0.161	0.160	1.64

arrival data collected by the two terminals was used to estimate the Earth-spacecraft range with decimeter precision [9], a precision orders of magnitude better than could be achieved with the spacecraft microwave Doppler data.

In late September 2005, a similar experiment was conducted by the same GSFC team to the Mars Orbiter Laser Altimeter (MOLA), an instrument on the Mars Global Surveyor (MGS) spacecraft in orbit about Mars. Because the MOLA laser was no longer operable following a successful topographic mapping mission at Mars, this was necessarily a one-way experiment in which the MOLA detector saw hundreds of pulses from a modestly powered Q-switched Nd:YAG laser at GSFC. The instrument parameters for these two experiments are summarized in Table 1.

It must be stressed that the latter were experiments of opportunity, not design. The near-infrared (NIR) detectors used in these experiments are far less sensitive than the photon-counting visible detectors typically used in SLR or LLR. As a result, the energy-aperture (EA) product needed to observe a return in these preliminary experiments, although modest, was significantly higher than would be necessary for a dedicated deep-space transponder mission. Furthermore, neither spacecraft had a capability of independently acquiring and locking onto the opposite terminal and instead relied on temporary illumination during the raster scan.

## 5 Testing Future Transponders/Lasercom Systems in Space

Interest at NASA in laser communications has been intermittently high since the 1960s and, with the recent successful transponder experiments, interest in laser transponders is on the rise as well. Past initiatives for interplanetary transponders or laser communications often were bogged down in esoteric

discussions on difficult topics such as the effects of atmospheric turbulence on beam propagation. It is well known that turbulence has several effects on laser beam propagation including beam spreading, short-term beam wander, and scintillation (fading) [2]. End-to-end ground-based experiments which can convincingly simulate all aspects of these complex systems are both difficult to envision and expensive to implement. Fortunately, atmospheric transmission and turbulence effects on the uplink and downlink beams are the same, whether the uplink beam is being reflected from a passive high altitude satellite in Earth orbit as in SLR/LLR or transmitted from a distant transponder or lasercom terminal in deep space. It may be relevant, therefore, to consider an experiment in which two closely spaced ground terminals range at different wavelengths to the same passive Earth-orbiting satellite as in Fig. 3. Each station must be located within the reflected return spot of the other station. The larger terminal, simulating the Earth station, would exchange reflected pulses from the satellite with a smaller station, simulating the remote transponder or lasercom terminal. In Fig. 3, we show SLR Station *A* ranging to a passive satellite (e.g., LAGEOS) in the infrared (1,064 nm) while Station *B* ranges to the same satellite in the green (532 nm). Each station is equipped with an additional receiver channel at the opposite wavelength to detect reflected pulses from the other station to simulate a dual wavelength transponder or lasercom experiment. The experiment is self-calibrating since the transponder measures the dogleg defined by Station *A*-satellite and Station *B*-satellite while the individual ranging systems measure the Station *A*-satellite and Station *B*-satellite

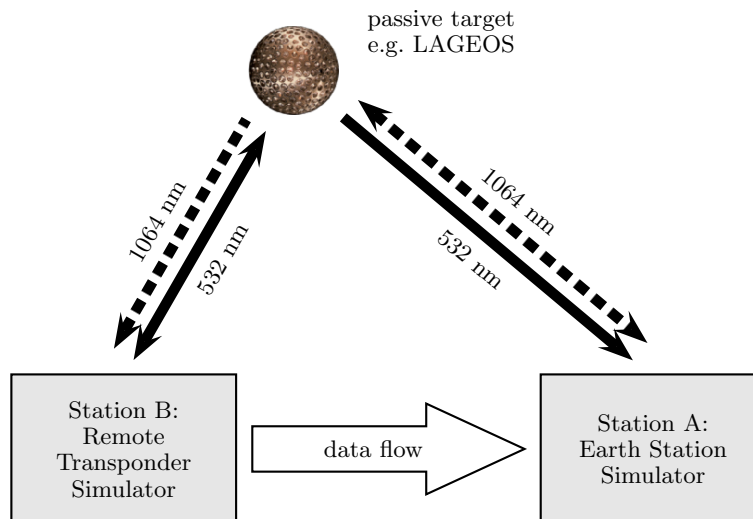


**Fig. 3.** Dual station laser ranging to LAGEOS with Station *A* simulating the Earth station and Station *B* simulating the remote transponder or lasercom terminal. Both stations must lie within each other's reflected spot.



distances and ground surveys typically define the interstation vector, or third leg of the triangle, to better than 2 mm. This provides an accurate way to test the ranging and time transfer algorithms. Automated acquisition of the Earth station by the remote terminal can be demonstrated by either turning off or ignoring the closed ranging loop at 532 nm while it searches for the reflected light at 1,064 nm. The ability to lock Station *A* onto the satellite via a closed single-ended ranging loop at 1,064 nm ensures a steady source of photons from the Earth station for the remote terminal to find and lock onto.

The link equations define the received signal strength at either station. For the infrared link from the Earth station *A* to the remote terminal *B* via a passive satellite, the link equation is given by [4]

$$\eta_R^{AB} = \frac{4\eta_q^B \eta_t^A \sigma_s \eta_r^B T_A^{2 \sec \theta_A} E_t^A A_r^B}{h\nu_A (\theta_t^A)^2 (4\pi)^2} \frac{E_t^A A_r^B}{R_R^4} \quad (3)$$

which depends on the transmitted energy  $E_t$ , the receive aperture  $A_r$ , the detector quantum efficiency  $\eta_q$ , the laser photon energy  $h\nu$ , the one-way zenith atmospheric transmission  $T_A$ , the satellite zenith angle  $\theta_A$ , the divergence half-angle of the laser beam  $\theta_t$ , the target optical cross-section  $\sigma_t$  (measured in square meters), and the optical throughput efficiencies of the transmitter ( $\eta_t$ ) and receiver ( $\eta_r$ ) optics, respectively. The *A* and *B* superscripts and subscripts indicate the terminal for which the value applies, and are reversed for the opposite link from terminal *B* to *A*. The quantity  $R_R$  is the slant range to the target satellite. For the nominally circular orbits of typical SLR targets,  $R_R$  can be expressed as a function of the satellite height above sea level  $h$ , and the satellite zenith angle

$$R_R(h, \theta_A) = -R_E \cos \theta_A + \sqrt{(R_E \cos \theta_A)^2 + h(h + 2R_E)}, \quad (4)$$

where  $R_E = 6,378$  km is the mean volumetric radius of the Earth and (4) reduces to  $h$  when  $\theta_A = 0$ .

For interplanetary transponder (or lasercom) links, the link equation is given by [4]

$$\eta_T^{AB} = \frac{4\eta_q^B \eta_t^A \eta_r^B T_A^{\sec \theta_A} T_B^{\sec \theta_B} E_t^A A_r^B}{h\nu_A (\theta_t^A)^2 (4\pi)^2} \frac{E_t^A A_r^B}{R_T^2}. \quad (5)$$

Setting the two mean signal counts equal in (3) and (5), we can derive an expression for the equivalent transponder distance,  $R_T$ , in terms of the actual slant range to the satellite,  $R_R$ , i.e.,

$$R_T(h, \theta_A, \sigma_s) = R_R^2(h, \cos \theta_A) \sqrt{\frac{4\pi T_B^{\sec \theta_B}}{\sigma_s T_A^{\sec \theta_A}}} \simeq R_R^2(h, \cos \theta_A) \sqrt{\frac{4\pi}{\sigma_s T_A^{\sec \theta_A}}}, \quad (6)$$

where the approximation holds if the remote terminal is in interplanetary cruise phase, in orbit, or sitting on the surface of a planet or moon with little

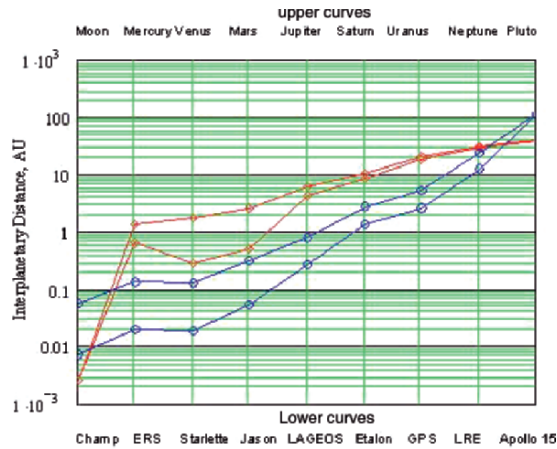


**Fig. 4.** The minimum and maximum distances from the Earth to the Moon and the eight planets listed at the top of the graph are illustrated by the *two upper curves* in the figure. The minimum and maximum transponder ranges simulated by the various SLR satellites listed at the bottom of the figure are indicated by the *two lower curves*.

or no atmosphere ( $T_B \sim 1$ ). Since the SLR satellites are normally tracked over the range  $0^\circ \leq \theta_A \leq 70^\circ$ , (6) defines a maximum and minimum simulated transponder range for each satellite. These are indicated by the blue curves in Fig. 4 for our selected satellites. In the plots, we have assumed a value  $T_A = 0.7$  corresponding to the one-way zenith transmission for a standard clear atmosphere at 532 nm. The red curves are plots of the minimum and maximum interplanetary distances of the Moon and other planets from Earth.

It is worthwhile to note that atmospheric turbulence can influence the effective transmitter beam divergence on the uplink, but this cancels out in our derivation of (6). Furthermore, the fading statistics for the dual station ranging experiment to the passive satellite should be comparable to that of an interplanetary transponder or lasercom experiment, at least to the extent that the satellite mimics a coherent point source of radiation.

Figure 4 shows that a dual station ranging experiment to the lowest of the SLR satellites, Champ, provides a weaker return than a two-way lunar transponder. Low elevation angle experiments to Jason are comparable to a Venus or Mars link when they are closest to Earth. Experiments to the LAGEOS and Etalon satellites would simulate ranging to Mercury, Venus, and Mars throughout their synodic cycles while experiments to GPS and LRE (at 25,000 km) would simulate links up to and beyond Jupiter and Saturn. Dual station experiments to the Apollo 15 reflector on the lunar surface would simulate transponder links to over 100 AU, well beyond the orbit of Pluto (<40 AU).

The nine SLR satellites in Fig. 4 were chosen based on their ability to simulate different transponder ranges and because the effects of target signa-

**Table 2.** Characteristics of selected SLR satellites which can be used to simulate deep-space transponder or lasercom links (from ILRS website).

Satellite	Altitude (km)	Mean target cross-section ( $10^6 \text{ m}^2$ )	Minimum transponder range (AU)	Maximum transponder range (AU)
Champ	500	1.0	0.007	0.057
ERS 1 and 2	800	0.85	0.02	0.135
Starlette–Stella	950	1.8	0.019	0.123
Jason	1,300	0.8	0.054	0.306
LAGEOS	6,000	15	0.263	0.771
GLOHASS	19,000	55	1.38	2.72
GPS	20,000	19	2.60	5.06
LRE (elliptical)	25,000	2	12.52	23.12
Apollo 15	384,000	1,400	111.6	

ture are minimized. The reduced pulse spreading by the target significantly improves the precision of the measured transponder range and also provides a reasonably high fidelity facsimile of the outgoing optical pulse train from a ground-based lasercom transmitter. The primary characteristics of these satellites, used in the computation of equivalent transponder ranges, are summarized in Table 2.

Another way to interpret Fig. 4 is to say that any *single* SLR station that can track the aforementioned satellites has demonstrated an adequate EA-product for the corresponding transponder link under the same noise background and atmospheric conditions. Since all of the ILRS stations are required to track LAGEOS for membership, they all have adequate EA-product to track out to about 1 AU. About a third of ILRS stations regularly track GPS, which from Fig. 4 or Table 2 implies an equivalent transponder range out to 5 AU. The workhorse NASA MOBLAS system, with an EA-product of  $0.045 \text{ J m}^{-2}$  and a power–aperture (PA) product of  $0.23 \text{ W m}^{-2}$ , falls into this category as does the photon-counting Graz station in Austria with EA and PA products of  $0.79 \times 10^{-5} \text{ J m}^{-2}$  and  $0.157 \text{ W m}^{-2}$ , respectively. As mentioned previously, three stations have routinely tracked the Apollo reflectors but only at night with low noise background and single photon returns. Nevertheless, the same EA-product, which is only about 70% larger than a MOBLAS, should permit transponder links beyond 100 AU under equivalent operating conditions.

## 6 Concluding Remarks

It is clear from the recent successes that decimeter or better interplanetary ranging and subcentimeter time transfer is within the current state-of-the-art and can be achieved with very modest laser powers and telescope apertures. These experiments of opportunity have bolstered interest at NASA in laser

transponders and laser communications. In a recent development, NASA's Lunar Reconnaissance Orbiter (LRO), tentatively scheduled for launch in 2008, will carry a small (21 mm diameter) telescope, with a relatively wide (1.15°) FOV, on its S-band microwave communications antenna. The latter will be used to view Earth-based SLR systems from lunar orbit. The incoming optical pulses at 532 nm will be transmitted from the focal plane of the telescope via fiber to one of the ranging detectors in the Lunar Orbiter Laser Altimeter (LOLA) instrument. The LOLA detectors, although designed primarily for the few nanosecond resolution altimetry channel at 1,064 nm, have sensitivity at 532 nm and will provide one-way differential range data to the altimetric mission, which requires highly accurate orbits for mapping the lunar topography and gravity field. Due to schedule constraints, there are no plans to put a transmitter on the LRO mission for full two-way transponding.

## References

1. J.J. Degnan: Satellite Laser Ranging: Current Status and Future Prospects, *IEEE Transactions on Geoscience and Remote Sensing*, **GE-23**, 398 (1985).
2. J.J. Degnan: Millimeter Accuracy Satellite Laser Ranging: A Review, in Contributions of Space Geodesy to Geodynamics: Technology, D.E. Smith and D.L. Turcotte (Eds.), *AGU Geodynamics Series* **25**, 133 (1993).
3. J.J. Degnan: Thirty Years of Satellite Laser Ranging, Proc. Ninth International Workshop on Laser Ranging Instrumentation, pp. 1–20, Canberra, Australia, November 7–11, 1994.
4. J.J. Degnan: Photon Counting Microlaser Rangers, Transponders, and Altimeters, Surveys in Geophysics, Special Issue on *Evolving Geodesy* **22**, 431 (2001).
5. J.J. Degnan: Asynchronous Laser Transponders for Precise Interplanetary Ranging and Time Transfer, Journal of Geodynamics (Special Issue on Laser Altimetry), pp. 551–594, November, 2002.
6. J.O. Dickey, P.L. Bender, J.E. Faller, X.X. Newhall, R.L. Ricklefs, J.G. Ries, P.J. Shelus, C. Veillet, A.L. Whipple, J.R. Wiant, J.G. Williams, and C.F. Yoder: Lunar laser ranging: a continuing legacy of the Apollo Program, *Science* **265**, 482 (1994).
7. T.W. Murphy Jr., J.D. Strasburg, C.W. Stubbs, E.G. Adelberger, L. Tom, A.E. Orin, E.L. Michelson, J. Battat, C.D. Hoyle, E. Swanson, and E. Williams: APOLLO: Meeting the Millimeter Goal, 14th International Workshop on Laser Ranging, San Fernando, Spain, June 7–11 (2004).
8. H.H. Plotkin, T.S. Johnson, P.L. Spadin, and J. Moye: Reflection of Ruby Laser Radiation from Explorer XXII, *Proc. IEEE* **53** 301 (1965).
9. D.E. Smith, M.T. Zuber, X. Sun, G.A. Neumann, J.F. Cavanaugh, J.F. McGarry, and T.W. Zagwodzki: Two Way Laser Link over Interplanetary Distance, *Science* **311**, 53 (2006).
10. X. Sun, G.A. Neumann, J.F. McGarry, T.W. Zagwodzki, J.F. Cavanaugh, J.J. Degnan, D.B. Coyle, D.R. Skillman, M.T. Zuber, and D.E. Smith: Laser Ranging between the Mercury Laser Altimeter and an Earth-based Laser Satellite Tracking Station over a 24 Million Kilometer Distance, presented at OSA Annual Meeting, Tucson, AZ, October 16–20, 2005.